

1 **A comparison of measured HONO uptake and release with**
2 **calculated source strengths in a heterogeneous forest**
3 **environment**

4
5 M. Sörgel^{1*}, I. Trebs², D. Wu³, and A. Held^{1,4}

6 1 University of Bayreuth, Atmospheric Chemistry, Bayreuth, Germany

7 2 Luxembourg Institute of Science and Technology, Environmental Research and Innovation
8 (ERIN) Department, Belvaux, Luxembourg

9 3 Max Planck Institute for Chemistry, Biogeochemistry Department, Mainz, Germany

10 4 Bayreuth Center of Ecology and Environmental Research, Bayreuth, Germany

11 * now at 3

12
13
14
15
16
17
18
19
20
21
22 Corresponding author:

23 Matthias Sörgel
24 Biogeochemistry Department
25 Max Planck Institute for Chemistry
26 P.O. Box 3060, 55020 Mainz, Germany
27 ++49-(0)6131-305-6401
28 m.soergel@mpic.de
29 <http://www.mpic.de/>

1 Abstract

2

3 Vertical mixing ratio profiles of nitrous acid (HONO) were measured in a clearing and on the
4 forest floor in a rural forest environment. For the forest floor, HONO was found to be
5 predominantly deposited, whereas net deposition was dominating in the clearing only during
6 nighttime and net emissions were observed during daytime. For selected days, net fluxes of
7 HONO were calculated from the measured profiles using the aerodynamic gradient method.
8 The emission fluxes were in the range of 0.02 to 0.07 $\text{nmol m}^{-2} \text{s}^{-1}$, and, thus were in the lower
9 range of previous observations. These fluxes were compared to the strengths of postulated
10 HONO sources. Laboratory measurements of different soil samples from both sites revealed
11 an upper limit for soil biogenic HONO emission fluxes of 0.025 $\text{nmol m}^{-2} \text{s}^{-1}$. HONO
12 formation by light induced NO_2 conversion was calculated to be below 0.03 $\text{nmol m}^{-2} \text{s}^{-1}$ for
13 the investigated days, which is comparable to the potential soil fluxes. Due to light saturation
14 at low irradiance, this reaction pathway was largely found to be independent of light intensity,
15 i.e. it was only dependent on ambient NO_2 .

16 We used three different approaches based on measured leaf nitrate loadings for calculating
17 HONO formation from HNO_3 photolysis. While the first two approaches based on empirical
18 HONO formation rates yielded values in the same order of magnitude as the estimated fluxes,
19 the third approach based on available kinetic data of the postulated pathway failed to produce
20 noticeable amounts of HONO. Estimates based on reported cross sections of adsorbed HNO_3
21 indicate that the lifetime of adsorbed HNO_3 was only about 15 min, which would imply a
22 substantial renoxification. Although the photolysis of HNO_3 was significantly enhanced at the
23 surface, the subsequent light induced conversion of the photolysis product NO_2 did not
24 produce considerable amounts of HONO. Consequently, this reaction might occur via an
25 alternative mechanism.

26 By explicitly calculating the HONO formation based on available kinetic data and simple
27 parameterizations we showed that a) for low NO_x the light induced conversion of NO_2 on
28 humic acids is light saturated already in the early morning, b) HONO formation from
29 photolysis of adsorbed HNO_3 should proceed via an alternative mechanism and c) estimates
30 of HONO emissions from soil are very sensitive to mass transfer and acidic soils do not
31 necessarily favour HONO emissions.

32

1 Introduction

Gaseous nitrous acid (HONO) may contribute up to ~ 80% to the primary formation of hydroxyl radicals (OH), which play a key role in the degradation of most air pollutants (Kleffmann et al., 2005, Kleffmann 2007; Volkamer et al., 2010). The source of OH radicals is the photolysis of HONO (R1):



The back reaction R2 consumes OH and regenerates HONO. R3 is typically a minor loss term for HONO (e.g., Su et al., 2008; Sörgel et al., 2011a; Oswald et al., 2014) and OH due to the low concentrations of both reaction partners. Solely considering R1 to R3 HONO is an OH radical reservoir as discussed for urban plumes (Lee et al., 2013). If R1 to R3 are in equilibrium, a photo stationary state (PSS) is established (e.g. Cox, 1974; Kleffmann et al., 2005). In case an additional efficient HONO loss term exists (e.g. deposition) (Harrison et al., 1996; Wong et al., 2011; Vandenboer et al., 2013), HONO formation would be a sink for OH radicals. For instance it was shown that plants (Schimang et al., 2006) and soils (Donaldson et al., 2014) efficiently take up HONO. However, if additional sources of HONO exist that exceed the loss terms; HONO is a source for OH radicals.

A well-known source of HONO is the heterogeneous disproportionation of NO₂, forming HONO and HNO₃:



Although reaction R4 is well-known, its mechanism is still unclear. A potential mechanism involving the dimer of NO₂ was proposed by Finlayson-Pitts and co-workers (Finlayson-Pitts et al., 2003), and has been further analysed using theoretical approaches (Miller et al., 2009; De Jesus Medeiros and Pimentel, 2011). This reaction was found to be too slow to explain daytime HONO mixing ratios well above the PSS (e.g., Kleffmann et al., 2005; Sörgel et al., 2011a; Wong et al. 2013). However, it is linked to the nighttime accumulation of HONO, which triggers early morning photochemistry (Alicke et al., 2003). Other light-independent mechanisms for NO₂ conversion to HONO, such as the reduction by organics (Gutzwiller et al., 2002) and chemisorption on mineral surfaces (Gustafsson et al., 2008) were also

1 proposed. All these reactions have not yet been quantified under field conditions and concerns
2 exist whether or not chemisorption would take place under environmental conditions
3 (Finnlayson-Pitts, 2009). Furthermore, NO₂ reduction on soot was found to be quickly
4 deactivated (Kleffmann et al., 1999; Arens et al., 2001; Aubin and Abbatt, 2007).

5 As the observed HONO mixing ratios almost always exceed those calculated from the PSS
6 assumption (summarized by Kleffmann (2007) and Volkamer et al. (2010)), numerous
7 attempts to identify HONO sources driven by light or by temperature that can overcome the
8 loss by photolysis were made. Recently, it was found that the heterogeneous
9 disproportionation (R4) can be catalysed by anions that are formed during photooxidation in
10 the atmosphere (Yabushita et al., 2009; Colussi et al., 2013). Lightenhancement of R4 has
11 also been attributed to HNO₃ photolysis (Ramazan et al., 2004), and photolysis of adsorbed
12 HNO₃ on natural surfaces was proposed as an important HONO source in the atmosphere
13 (Zhou et al., 2002; Zhou et al., 2003; Zhou et al., 2011).

14 In contrast to HONO formation observed on natural surfaces (Zhou et al., 2003, Zhou et al.,
15 2011), HONO has not been detected as a primary reaction product of HNO₃ photolysis in
16 laboratory studies up to now (Zhu et al., 2010, Schuttlefield et al., 2008, Rubasinghege and
17 Grassian, 2009; Abida et al., 2012). Most studies (Zhu et al., 2010, Schuttlefield et al., 2008,
18 Abida et al., 2012) report NO and NO₂ as the main products of this reaction (Rubasinghege
19 and Grassian, 2009). The formation of NO₂ and NO₂* is also proposed for an alternative
20 mechanism, which involves photolysis of complexes of either HNO₃ or NO₃⁻ and NO₂ or
21 N₂O₄, respectively (Kamboures et al., 2008). Recent studies applying a novel laser-based
22 technique (Zhu et al., 2010, Abida et al., 2012) identified excited NO₂* as the main photolysis
23 product of adsorbed HNO₃, and, furthermore confirmed an enhanced absorption cross section
24 of adsorbed HNO₃ compared to gas phase HNO₃. Potentially, NO₂* reacting with water
25 vapour can produce HONO, but this reaction does not result in significant amounts of HONO
26 under atmospheric conditions (Crowley and Carl 1997; Sörgel et al., 2011a; Amedro et al.,
27 2011). Hence, Zhou et al. (2011) suggested that NO₂ formed during HNO₃ photolysis further
28 reacts via the mechanism proposed by Stemmler and co-workers (Stemmler et al., 2006;
29 Stemmler et al., 2007), where solid organic material like humic acids (HA) acts as a
30 photosensitizer and reduces NO₂ (George et al., 2005). Photosensitized reactions may be a
31 promising pathway for explaining daytime HONO formation as hypothesized from
32 correlations of the unknown HONO source with the photolysis frequency of NO₂, $j(\text{NO}_2)$, or
33 irradiance (e.g. Su et al., 2008; Sörgel et al., 2011a; Wong et al., 2012). The photolysis of o-

1 nitrophenols was also proposed as a HONO source (Bejan et al., 2006) that, however, has not
2 yet been quantified in field measurements. As it depends on the amount of nitrophenols in air,
3 this source is expected to be more important for polluted urban conditions (Bejan et al., 2006).
4 A process directly driven by temperature could be the volatilization of HONO from soil nitrite
5 (Kubota and Asami, 1985; Su et al. 2011). The temperature dependence of this process has
6 been attributed to the temperature dependence of the Henry's law equilibrium between soil-
7 solution and soil-air (Su et al., 2011). Additionally, it was suggested that HONO emissions
8 are driven by ammonia oxidizing bacteria in soil, whose activity also depends on temperature
9 (Oswald et al., 2013). Nitrogen availability for microorganisms was found as a limiting factor
10 for HONO emissions from natural soils (Malianen et al., 2013). HONO deposition during
11 night and reemission that is driven by acid displacement (VandenBoer et al. 2015) during
12 daytime has been proposed to explain the missing daytime source (VandenBoer et al. 2013).
13 The physicochemical interactions with soil particles have been analysed in more detail by
14 Donaldson et al. (2014 a, b).

15 Regardless of the mechanism, the ground surface has been proposed as a major source of
16 HONO (e.g. Febo et al., 1996; Stutz et al., 2002; Zhang et al., 2009; Sörgel et al., 2011b;
17 Wong et al., 2012, Wong et al. 2013, VandenBoer et al., 2013), although there is a potential
18 contribution from other heterogeneous sources within the boundary layer (Zhang et al., 2009;
19 Wong et al., 2013). Flux measurements of HONO (Zhou et al., 2011; Ren et al., 2011)
20 reported strong daytime upward fluxes, thus confirming a ground source. Contrarily, a recent
21 study (Li et al., 2014) based on concentration measurements of HONO in the residual layer
22 and the mixed layer proposed that an internal recycling mechanism (reaction between NO_x
23 and HO_x) is mainly responsible for HONO formation.

24 In this study, we present vertical mixing ratio profiles of HONO measured close to the ground
25 surface (< 2 m) in a clearing and on the forest floor in a heterogeneous forest landscape in
26 order to identify sources and sinks of HONO in natural environments. Under favourable
27 conditions, our setup can be used to derive estimates of the surface fluxes of HONO by the
28 aerodynamic gradient method. These fluxes are compared to best estimates of HONO source
29 strengths of three proposed mechanisms derived from measured quantities: a) soil HONO
30 emissions, b) photosensitized NO_2 conversion, and c) HNO_3 photolysis.

31

2 Experimental

Vertical mixing ratio profiles of HONO, nitrogen oxides (NO_x), and ozone were measured in a clearing and on the forest floor at the Waldstein ecosystem research site in the Fichtelgebirge mountains, NE Bavaria (Germany) in 2011 and 2012 as part of the research project “Exchange processes in mountainous regions (EGER),” Foken et al. (2012). The profile measurements were made in June/July 2011 (intensive observation period IOP-3) in the clearing “Köhlerloh” ($50^\circ 08' 22.3''$ N, $11^\circ 52' 01.5''$ E), and in August/September 2012 (IOP-4) on the forest floor about 290 m north of the clearing site close to the main tower ($50^\circ 08' 31.2''$ N, $11^\circ 52' 00.8''$ E; 775 m a.s.l.) of the “Weidenbrunnen” site. Meteorological variables for the comparison of both campaigns were taken from the “Pflanzgarten” site, which is 280 m north-west of the main tower and 490 m north north-west of the clearing site. An aerial view of the different sites can be found in the Supplement (Fig. S1).

HONO was measured using a commercially available long path absorption photometer (LOPAP, QUMA, Wuppertal, Germany) with a time resolution of 3 minutes. A detailed description of the instrument is provided by Heland et al. (2001) and Kleffmann et al. (2002). The instrument was placed on a scaffold in a ventilated aluminium box as described by Sörgel et al. (2011b). The limit of detection (3σ of zero air noise) ranged from 1 to 7 ppt. NO and NO_2 were measured by chemiluminescence (Model 42i-TL Thermo Scientific, Franklin, MA, USA) using a specific photolytic converter for NO_2 (Droplet Measurement Technologies, Boulder, Co, USA). The limit of detection was 50 ppt for NO and about 140 ppt for NO_2 . Trace gas profiles of HONO, NO, and NO_2 were obtained by moving the external sampling unit of the LOPAP and an inlet line for NO_x to five (0.1 m, 0.2 m, 0.4 m, 0.8 m and 1.6 m) or three (0.1 m, 0.4 m and 1.6 m) different heights using an automated lift system (Fig. S2). The dwell time at each height was 6 and 7 min in IOP-3 and 9 min (IOP-4), which allowed sufficient sampling periods with respect to the time resolution of the LOPAP (1-2 data points). All data of the lift system (NO_x , HONO, temperature and lift position) were recorded every 20 sec. Additionally, eddy covariance measurements were made during IOP-3 with a CSAT3 sonic anemometer (Campbell Scientific, Logan, UT, USA) located at a height of 2.25 m on a mast about 20 m north-west of the profile measurements. During IOP-4, a Young sonic anemometer (Model 81000, R.M. Young, Traverse City, MI, USA) was located about 2 m east of the profile measurements at a height of 2 m. The friction velocity (u^*) was calculated with the TK3 software (Mauder and Foken, 2011). Air temperature was measured

1 by radiation shielded and ventilated Pt-100 sensors with a resolution of 0.1 K at 1.4 m (1.6 m
2 in IOP-4) and 0.1 m above ground level. Soil temperature was monitored with a Pt-100 sensor
3 at a depth of 2 cm.

4 At the “Pflanzgarten” site, air temperature and relative humidity (RH) were measured with
5 HMP45 sensors (Vaisala, Helsinki, Finland) at a height of 2 m, precipitation was measured
6 with an OMC-212 rain gauge (Observator instruments, Ridderkerk, The Netherlands), and
7 solar global irradiance was measured on the roof of the measurement container with a CM5
8 pyranometer (Kipp and Zonen, Delft, The Netherlands). The HONO photolysis frequency
9 $j(\text{HONO})$, was calculated from global radiation according to Trebs et al. (2009).

10 Spectral irradiance and photolysis frequencies were calculated using the Tropospheric
11 Ultraviolet and Visible (TUV) radiation model (Madronich and Flocke, 1998) version 5.0.
12 Additional information about methods and instruments can be found in the supplementary
13 material.

14

15 **3 Results and discussion**

16 ***3.1 Meteorological conditions and comparison of sites***

17

18 As shown in Fig. 1, the range of air temperature at the “Pflanzgarten” site was comparable for
19 both campaigns and ranged between about 5 °C and 27 °C. The maximum temperatures were
20 27.3 °C for IOP-3 and 25.8 °C for IOP-4, respectively. The minimum temperature of the
21 June/July period (IOP-3) was lower (5.5 °C) than during IOP-4 in September (6.0 °C). Mean
22 values (and standard deviations) were 14.7 ± 5.1 °C for IOP-3 and 14.2 ± 4.4 °C for IOP-4.
23 Accordingly, RH values cover similar ranges from about 30 % to 100 % with somewhat
24 higher values in the summer campaign due to frequent rain events (i.e. an average
25 precipitation of 1.8 mm d^{-1} in IOP-3 and 0.3 mm d^{-1} in IOP-4). The long-term monthly means
26 (1971-2000) at this site are 3.6 mm d^{-1} for June, 4.1 mm d^{-1} in July and 2.8 mm d^{-1} in
27 September (Foken, 2003). Consequently, both periods exhibited less precipitation than the
28 long term average, although frequent but light rain events occurred during IOP-3, whereas in
29 September (IOP-4) precipitation events were rare. Maximal RH values are slightly different
30 for the two IOPs and range from 95 % to ~ 100 %. The values greater than 100 % have to be
31 viewed with caution as the sensor accuracy in the range from 90 % RH to 100 % RH is ± 3 %
32 and the sensor is not able to measure accurately if water is condensing at high humidity.

1 Global radiation, and thus $j(\text{HONO})$, were higher in June/July 2011 than in September 2012.
2 Correspondingly, the calculated $j(\text{HONO})$ values show a maximum of $2 \times 10^{-3} \text{ s}^{-1}$ in 2011 and
3 $1.8 \times 10^{-3} \text{ s}^{-1}$ in 2012. The radiation and photolysis frequencies at the forest floor are a factor
4 of 10 to 40 lower than above the canopy depending on the time of day and canopy structure
5 (Sörgel et al., 2011b). $J(\text{HONO})$ values calculated by applying a factor of 10 are shown in
6 Fig. 1d. Since weather conditions were comparable, major differences between the two
7 campaigns are expected to be due to a) availability of radiation, b) turbulent exchange and c)
8 groundcover. Radiation and turbulent exchange are reduced at the forest site below the
9 canopy compared to the open clearing. The ground cover at the clearing was dominated by
10 grass and blueberry, while the forest floor was mainly covered by moss.

11

12 **3.2 HONO mixing ratio differences and estimated net fluxes**

13

14 NO mixing ratios at the 1.6 m level were generally low, especially during nighttime. Average
15 mixing ratios were 0.2 ppb during the first period in 2011 (Fig. 2a), 0.1 ppb during the second
16 period in 2011 (Fig. 2b), and 0.05 ppb in 2012 (Fig. 3a). Due to the well-known soil NO
17 emissions (e.g., Ludwig et al., 2001; Bargsten et al., 2010) caused by microbiological activity,
18 NO mixing ratios were higher at 0.1 m. The average mixing ratios close to the ground (Figs.
19 S3 to S5) at 0.1 m were 0.75 ppb during the first period, 0.5 ppb during the second period in
20 2011, and 0.1 ppb in 2012. Average NO₂ mixing ratios at the upper level were 1.7 ppb (min.
21 0.3 ppb and max. 3 ppb) during the first period, 1.1 ppb (min. 0.2 ppb and max. 2.4 ppb)
22 during the second period in 2011, and 1.6 ppb (min. 0.2 ppb and max. 4.8 ppb) in 2012.
23 Average HONO mixing ratios at the 1.6 m level were 94 ppt (min. 12 ppt and max. 308 ppt)
24 during the first period, 80 ppt (min. 30 ppt and max. 316 ppt) during the second period in
25 2011, and 90 ppt (min. 26 ppt and max. 257 ppt) in 2012.

26 Since vertical mixing ratio differences are the result of the competition between sources and
27 sinks as well as of transport dynamics, Fig. 2 and Fig. 3 additionally show vertical
28 temperature differences and the friction velocity u^* . Temperature differences reflect
29 atmospheric stability and u^* is a measure of the intensity of turbulent exchange. A typical
30 diurnal cycle caused by radiative heating and cooling of the surface was observed at the
31 clearing, with stable conditions (positive temperature differences) during the night and
32 unstable conditions during the day. The temperature differences between 0.1 m and 1.4 m

1 above the ground were up to 6 K during the night and up to -4 K during the day. During stable
2 conditions, u^* dropped and mixing ratio differences increased due to suppressed transport. In
3 the clearing, very stable and calm conditions caused large HONO and NO (not shown) mixing
4 ratio differences during sunset. Below the canopy at the forest site, diurnal cycles of stability
5 are typically opposite to those observed at the clearing (Foken, 2008). However, the observed
6 temperature differences do not feature a clear diurnal pattern and differences are generally an
7 order of magnitude lower than at the clearing. This can be explained by the reduced heating of
8 the forest floor and the reduced radiative cooling due to the shading of the canopy. As
9 windspeed is reduced by the canopy as well, the friction velocity is on average a factor of
10 three to four lower. Maximal values of u^* were 0.46 m s^{-1} in the clearing and 0.16 m s^{-1} on the
11 forest floor, respectively. HONO differences in the clearing (1.6 m to 0.1m) shown in Figs.
12 2c,d feature distinct diurnal cycles with positive gradients at night indicating net deposition
13 and negative gradients during day indicating net emission. On the forest floor, HONO
14 differences were either positive or close to zero, i.e. net emission was not observed (Fig. 3b).

15

16 We calculated net HONO fluxes from selected profiles using the aerodynamic gradient
17 technique (cf. Wolff et al., 2010). Despite the fact that u^* was measured at 2.25 m on a
18 separate tower about 20 m from the profile measurements at the clearing, the measurements
19 were influenced by the same ground cover (dimensions of clearing $\sim 300 \times 400 \text{ m}$). At the
20 forest floor both measurements were collocated ($\sim 2 \text{ m}$ distance and u^* measured in 2 m
21 height). Mixing ratio differences were considered to be representative for the air layer
22 between 1.6 m and 0.1 m at the forest floor, but at the clearing differences between 1.6 m and
23 0.4 were taken as 0.1 m was below the zero plane displacement height (d).

24 The calculated daytime net emission fluxes of HONO at the clearing were in the range of 0.01
25 to $0.07 \text{ nmol m}^{-2} \text{ s}^{-1}$ (mean $0.04 \pm 0.02 \text{ nmol m}^{-2} \text{ s}^{-1}$; $N=17$). This is about a factor of three
26 lower than fluxes reported for another rural forested site (Zhou et al., 2011; Zhang et al.,
27 2012) and about an order of magnitude lower than for semi-rural and urban sites (Harrison
28 and Kitto 1994; Harrison et al. 1996; Ren et al., 2011). However, these fluxes are higher than
29 the values observed at Blodgett Forest (Ren et al., 2011). The mean HONO net emission flux
30 estimate of $0.04 \text{ nmol m}^{-2} \text{ s}^{-1}$ with a corresponding mixing ratio of 65 ppt at 1.6 m at the
31 clearing compares reasonably well with the somewhat lower fluxes at Blodgett Forest (flux $<$
32 $0.01 \text{ nmol m}^{-2} \text{ s}^{-1}$; 20-30 ppt) and with the somewhat higher fluxes at the PROPHET site
33 (mean flux $0.19 \text{ nmol m}^{-2} \text{ s}^{-1}$; 70 ppt). The low fluxes at Blodgett Forest have been attributed

1 to the alkalinity of the soil, which, according to acid- base and Henry's Law equilibrium (Su et
2 al., 2011), should enhance HONO uptake or hinder the release. The calculated fluxes indicate
3 the existence of a daytime ground source, whose strength is comparable in order of magnitude
4 to that found in other studies in rural forested areas. Nighttime net deposition fluxes ($0.006 \pm$
5 $0.003 \text{ nmol m}^{-2} \text{ s}^{-1}$; $N = 12$) were about a factor of seven lower than daytime net emission
6 fluxes at the clearing (see Sect. 3.3.1).

7 At the forest floor, only net deposition was observed with fluxes varying between zero and
8 about $0.012 \text{ nmol m}^{-2} \text{ s}^{-1}$ (mean: 0.004 ± 0.003 ; $N = 52$) for the selected days (4 -7 Sep 2012).
9 Hence, net deposition fluxes at the forest floor were comparable to nighttime net deposition at
10 the clearing. Assuming that daytime deposition fluxes at the clearing are within the same
11 range, emission fluxes at the clearing are at least about 15 % higher than the net fluxes. If
12 considerable stomatal uptake of HONO, as proposed by Schimang et al. (2006), occurs, the
13 daytime deposition would be much higher than during nighttime due to stomatal aperture.
14 Hence, to sustain the observed net emission fluxes, the HONO emission from the ground
15 would be even higher.

16 It should be noted that the derived fluxes should be considered as rough estimates for several
17 reasons. The profiles were measured sequentially and not simultaneously at the different
18 heights. Hence, only profiles under stationary conditions were evaluated, i.e. when mixing
19 ratio changes between two profile cycles were small at each measurement height. This was
20 mainly the case from 22:00 to 4:00 during night and from 11:00 to 15:00 during day.
21 Furthermore, the mixing ratio differences during daytime were rather small (5 to 26 ppt; mean
22 14 ppt). The differences were 1.3 to 8.5 times the standard deviation of the mean values at one
23 height and larger than the combined errors (sum of standard deviations of both heights).
24 Differences that were smaller than the combined standard deviation were omitted for the flux
25 calculations. Besides the uncertainty in the mixing ratio differences, the estimate of the zero-
26 plane displacement height d has considerable influence on the fluxes. We used $d = 0.7$ times
27 the canopy height (Foken, 2008) with a canopy height of 0.25 m of the surrounding blueberry
28 canopy (Falge, 2014 personal communication) at the clearing. As roughness elements (like
29 dead wood, blueberry, small spruce and grass) were distributed very inhomogeneously, it is
30 unclear if the applied displacement height is appropriate and would hold for all wind
31 directions. If the canopy height would have been chosen as 0.4 m instead, the fluxes would
32 decrease by about 20 %. Compared to the error of the mixing ratio differences and of the
33 displacement height, the error in u^* is expected to be negligible. At the forest floor we

1 measured at a flat surface covered with moss that has a comparably low roughness ($d = 0.007$
2 m), thus the fluxes are less sensitive to small differences in d .

4 **3.3 HONO sinks**

5 **3.3.1 Deposition**

6
7 Except for the uptake of HONO by aerosol surfaces, no considerable gas phase HONO sinks
8 exist in the absence of light. This implies that dry and wet deposition are the most important
9 loss pathways in the dark.

10 Net deposition means that although HONO formation by either heterogeneous
11 disproportionation of NO_2 or direct soil emission may take place, net deposition is observed
12 because the production of HONO is smaller than the loss by deposition. For our study, soil
13 emissions can be neglected (see 3.4.1). Calculated nighttime deposition velocities of 0.08 to
14 0.5 cm s^{-1} (mean 0.24 ± 0.13) at the clearing were in the lower range of reported values at
15 0.08 to 6 cm s^{-1} (Harrison and Kitto 1994; Harrison et al., 1996; Stutz et al., 2002).

16 At the forest floor, deposition was the dominating process during day and night. The vertical
17 profiles (Fig. 3b) do not provide evidence that HONO emission from the ground surface takes
18 place because the differences are either positive or ambiguous within the uncertainty range.
19 The HONO deposition velocities ranged from 0.03 to 0.4 (mean $0.16 \pm 0.08 \text{ cm s}^{-1}$), which is
20 in the lower range of previously reported values (e.g., Harrison et al., 1996, Stutz et al., 2002)
21 and a factor of 1.5 lower than at the clearing. To our knowledge, measured HONO fluxes at
22 forest floors have not been reported up to now.

23 In a modelling study, Wong et al. (2011) pointed out that nighttime deposition is an important
24 part of HONO cycling, which was recently confirmed by vertical profile measurements
25 (VandenBoer et al., 2013). VandenBoer et al. (2013) proposed that the deposited HONO
26 might form a reservoir that is re-emitted during the day, and, can thus explain a significant
27 fraction of the missing daytime source. For the forest floor, we can exclude this pathway as a
28 general source of HONO because no emissions were observed. This is in line with laboratory
29 studies, which showed that HONO can be taken up by plants (Schimang et al., 2006) and soil
30 (Donaldson et al., 2014). Due to the limited available data we cannot exclude that re-emission
31 may occasionally take place. However, we showed that net deposition (even if it is small)
32 persists during the day at the forest floor during our measurement period. Thus, sources and

1 sinks coexist over small spatial scales, which has to be taken into account for measurements at
2 elevated levels that integrate over larger areas (horizontal heterogeneity), as well as for
3 measurements above the canopy (vertical heterogeneity).
4

5 **3.3.2 Photolysis**

6
7 Photolysis has been identified as the dominating HONO loss process during the day (e.g.,
8 Kleffmann, 2007; Su et al., 2008; Sörgel et al., 2011a; Wong et al., 2013; VandenBoer et al.,
9 2013; Oswald et al., 2014). We calculated the HONO loss rates from photolysis frequencies
10 and HONO mixing ratios within a boundary layer height of 1000 m in two different ways: (a)
11 the measured HONO mixing ratio at 1.6 m was used for the entire volume or, (b) assuming a
12 linear HONO profile throughout the boundary layer to account for elevated HONO levels
13 close to the ground as observed by Zhang et al. (2009) and VandenBoer et al. (2013). The
14 artificial linear HONO profile was created using the measurements at 1.6 m and a background
15 level (free troposphere) of 10 ppt (Zhang et al., 2009). The geometric mean of these values
16 was used to calculate the HONO loss within the boundary layer volume. Using these two
17 simplified approaches yields loss rates of (a) 0.2-1 ppb h⁻¹ and (b) 0.08-0.5 ppb h⁻¹. These
18 values are within the range of values reported for the unknown HONO source (e.g. Kleffmann
19 2007). This is not surprising because the photolytic loss and the unknown source were found
20 to be the dominant terms of the HONO budget for low NO_x levels (e.g., Sörgel et al., 2011a;
21 Oswald et al., 2014), i.e. in the absence of other sources and sinks the photolytic loss equals
22 the unknown source. Integrating the photolytic loss term over a boundary layer height of 1000
23 m and converting it into a surface flux yields mean fluxes of (a) 4.6 nmol m⁻² s⁻¹ and (b)
24 2 nmol m⁻² s⁻¹ respectively, which is a factor 100 and 40 higher than the mean emission flux
25 derived from the measurements at the clearing (see Sect. 3.2). Consequently, the contribution
26 of the surface emissions to the HONO source would be in the order of a few percent. This is
27 in agreement with a proposed internal volume source (Li et al., 2014) and estimates of ground
28 source contributions of about 20 % derived from measured boundary layer profiles (Zhang et
29 al., 2009; Li et al., 2014). Close to the ground (lowest 35 m) a contribution of more than 60 %
30 was found in modelling studies (Czader et al., 2012; Wong et al. 2013). As these studies were
31 conducted in the urban area of Houston (Texas, USA), which is characterized by higher direct
32 HONO emissions and higher levels of NO_x compared to our site, the relative contribution of
33 the ground source in the lowest 35 m might be higher for our site. Nevertheless, the
12

1 contribution was reduced to about 50 % by integrating the lowermost 300 m (Wong et al.,
2 2013), and, therefore integrating over a boundary layer height of 1000 m will further reduce
3 this contribution. As none of the other boundary layer profile measurements have been
4 analysed with a chemistry-transport model up to now, it remains unclear if the differences in
5 HONO budgets (ground versus gas phase) are real or are caused by the different assumptions
6 and simplifications in the different approaches.

8 **3.4 HONO ground sources**

9
10 The existence of a HONO ground source was confirmed by profile (e.g., Zhang et al., 2009;
11 VandenBoer et al., 2013) and flux measurements (Zhou et al., 2011; Ren et al., 2011). In the
12 following we compare the measured ground source to estimates for three different proposed
13 formation mechanisms based on measured quantities.

14 **3.4.1 Soil emissions**

15
16 For both the forest and the clearing site, a set of soil samples was collected from two different
17 ground cover types and potential HONO emission fluxes were measured using a dynamic
18 chamber in the laboratory (for details see Appendix). HONO fluxes were mostly within the
19 calculated uncertainty range (Fig. S6). The sample taken directly below the lift system at the
20 clearing (sample 4, Fig.S6) was the only sample for which potential emissions were observed.
21 From those measurements we derive an upper limit for the HONO soil emission flux of 0.025
22 ± 0.015 $\text{nmol m}^{-2} \text{s}^{-1}$. This flux also represents an upper limit with regard to the experimental
23 conditions as the chamber was flushed with zero air and the samples were measured at 25 °C.
24 During the field measurements, the soil temperature at 2 cm depth did not exceed 20 °C at the
25 clearing. Comparison of the maximal fluxes measured in the laboratory (0.025 $\text{nmol m}^{-2} \text{s}^{-1}$)
26 with maximal fluxes calculated from soil nitrite ($0.35 - 0.99$ mg kg^{-1} in terms of N) and pH
27 ($3.0 - 3.4$) values ($F(\text{HONO}_{\text{max}}) = 1810$ $\text{nmol m}^{-2} \text{s}^{-1}$) according to Su et al. (2011) reveals that
28 the measured fluxes are at least four orders of magnitude lower. For the calculations we used
29 a gravimetric soil water content of $\vartheta_{\text{soil}} = 0.2$ kg kg^{-1} , a transfer velocity (v_{tr}) of 1 cm s^{-1} (Su et
30 al., 2011) and measured pH and nitrite values (see Table S1). The discrepancy between our
31 measurements and the calculations according to Su et al. (2011) reduces to about a factor of
32 50 when v_{tr} is determined for our measurement setup instead of using a fixed value of 1 cm s^{-1}

1 ¹. The transfer velocity v_{tr} was determined by calculating the soil resistance according to
2 Moldrup et al. (2000) from measured soil properties for the Waldstein site (Bargsten et al.,
3 2010) and using the aerodynamic resistance ($R_{aero} = 90 \text{ s m}^{-1}$) from a chamber system of
4 similar design and dimensions (Pape et al., 2009). This comparison emphasizes the
5 importance of explicitly considering mass transfer between the soil and atmosphere.
6 Additionally, based on soil nitrite ($\sim 1 \mu\text{g g}^{-1} \text{N}$) and pH (~ 3) values at our site, one would
7 expect rather high HONO emissions according to the acid base and Henry's law equilibrium.
8 Hence, it seems more likely that microbes are directly involved in the HONO formation as
9 proposed by Oswald et al. (2013), but microbial activity in our samples was low due to the
10 low pH (~ 3) of the organic soil (e.g., Matthies et al., 1997; de Boer and Kowalchuk, 2001
11 and Rousk et al., 2010). Maljanen et al. (2013) found that some acidic forest soils emit
12 measurable amounts of HONO and, thus, proposed nitrogen availability for the microbes as
13 an important factor controlling HONO emissions. The mechanisms controlling HONO
14 emissions from soils (microbial production versus physicochemical release) are still under
15 debate. Maximum emissions for neutral to alkaline soils were attributed to the activity of
16 ammonium oxidizing bacteria (Oswald et al. 2013). Donaldson et al. (2014b) studied the effect
17 of surface acidity of soil particles (in contrast to the bulk soil pH) on HONO uptake. Their
18 study confirmed that rather the acidity of the particles than the bulk pH determined the
19 HONO exchange, which could explain HONO emissions at high (bulk) pH. Nevertheless, this
20 mechanism is applicable to mineral soils only. Another possible effect would be HONO loss
21 in the soil by chemodenitrification as proposed by Clark (1962). During chemodenitrification
22 in the soil, HONO is converted to NO and N_2O depending on pH and organic content with the
23 highest conversion rates at low pH and high organic content (e.g. Allison 1963, van Cleemput
24 and Baert 1984; Ventera et al., 2005). A recent flow tube study (Donaldson et al., 2014a)
25 reports 16 % NO and 13 % N_2O yield from HONO adsorbing to a mineral soil (less than 3 %
26 organic and pH of 6.5). Thus, based on the prior semi quantitative studies high loss rates
27 could be expected for the organic soil at our site. Therefore, the acidic conditions of the
28 organic soil at the Waldstein site may lead to additional HONO loss by chemodenitrification
29 and, thus, low soil HONO emissions.

30
31

3.4.2 Light-induced NO₂ conversion

HONO fluxes from light-induced NO₂ conversion were calculated by assuming that the flux from the surface equals the chemical formation at the surface. HONO is formed by reactive collisions of NO₂ with the humic acid surface, and Stemmler et al. (2007) defined their uptake coefficient (γ_{rxn}) as the ratio of these reactive collisions to the number of gas-kinetic collisions of NO₂ molecules with the surface. Hence, we calculated the HONO flux by multiplying the number of gas kinetic collisions given by Eq. (1) with the reactive uptake coefficient given by Eq. (2) (Stemmler et al., 2007):

$$Z_w = \frac{n \times \omega}{4} \quad (1)$$

$$\gamma_{rxn} = \frac{4}{\omega} \times \frac{1}{9.3 \times 10^{22} \times [NO_2] \times [F]^{-1} + 2330} \quad (2)$$

where Z_w is the number of collisions per time (s) and area (m²), n is the volume number density per m³, ω is the mean thermal velocity of NO₂ in m s⁻¹, [NO₂] is the NO₂ mixing ratio in ppb measured at 10 cm above the surface, and F is the actinic flux in the 400-750 nm range in photons per m³ and s⁻¹. For simplicity, we used the irradiance in the 400-700 nm range (equivalent to the photosynthetic active radiation (PAR)) instead of the actinic flux from 400-750 nm for F because this value can be directly compared to measurements and to the model output of the TUV. Furthermore, in the study of Stemmler et al. (2007) the actinic flux of the lamps and absorption of the humic acid was low in the 700-750 nm wavelength range, thus having a small influence on the reactive uptake. Since our simple model assumes a flat surface of 1 m² completely covered with humic acid, it is well justified to use the irradiance instead of the actinic flux.

Calculation of the HONO flux using equations 1 and 2 with NO₂ mixing ratios measured 10 cm above the surface and modelled irradiance resulted in light-saturation of HONO formation in the early morning at about 7:00 CET and it remains independent of light intensity for most of the day (see Fig. 4). In addition, the saturation itself is dependent on NO₂ with the fastest saturation observed for low NO₂ mixing ratios. Stemmler et al. (2006) explain this behaviour by two competing processes: a) the light driven formation of the “reductive centres” that react with NO₂ and b) the competing light driven formation of oxidants that deactivate these reductive centres. If more NO₂ is available at the surface the reaction rate increases and the deactivation rate decreases. A saturation of the surface with respect to NO₂ is observed for

1 mixing ratios > 50 ppb (Stemmler et al., 2006; Stemmler et al., 2007). If this saturation
2 behaviour (with respect to light intensities) also prevails on natural surfaces, at mixing ratios
3 below 1 ppb the unknown HONO source should be solely correlated with NO₂ independent
4 from radiation, which to our knowledge has not been reported up to now. Previous studies
5 found that the unknown HONO source correlated with $j(\text{NO}_2)$ or irradiance with only a minor
6 dependence on NO₂ (e.g., Su et al., 2008; Sörgel et al., 2011a; Wong et al., 2012). However,
7 the type and structure of photosensitizers on natural surfaces might differ substantially from a
8 pure humic acid film and, thus, might not be saturated at high light intensities. For example
9 for humic acid dissolved in ice, Bartels-Rausch et al. (2010) did not observe deactivation of
10 the surface uptake. However, only actinic fluxes of up to about 100 W m⁻² (400-700 nm) were
11 considered, compared to irradiance values of about 400 W m⁻² in the same wavelength range
12 around noon in our study. Consequently, we consider the lightsaturation of NO₂ conversion
13 on organic surfaces as a key issue for determining the role of this HONO formation pathway
14 in the environment.

15

16 **3.4.3 Photolysis of adsorbed HNO₃**

17

18 The photolysis of HNO₃ adsorbed to surfaces has also been suggested as a source of HONO
19 (e.g., Zhou et al., 2002; Zhou et al., 2011). We measured the leaf nitrate loadings of young
20 spruce trees (up to 1.6 m height) at the clearing close to the HONO measurement setup. A
21 detailed description of the sampling and the calculations can be found in the supplementary
22 material. Unfortunately, measurements of the nitrate loadings on the grass below the HONO
23 inlets are not available, but we assume that they are comparable to the nitrate loadings of the
24 trees. Nitrate loadings at the forest site were not measured, but the contribution of HNO₃
25 photolysis is expected to be much lower than at the clearing as the available radiation is
26 attenuated by the canopy by a factor of about 10 – 25 (Sörgel et al., 2011b). Furthermore, we
27 have found no evidence for a HONO source at the forest floor (cf. Sect. 3.2).

28 The nitrate loadings of the young spruce trees at the clearing are $1.7 \pm 0.7 \times 10^{-5}$ mol m⁻²,
29 which is in relatively good agreement with the value of $0.8 \pm 0.3 \times 10^{-5}$ mol m⁻² reported by
30 Zhou et al. (2011). Both research sites are located in rural forested areas, but considering the
31 influence of different environmental variables, such as NO_x mixing ratios, precipitation
32 intensity and plant surfaces, all of which influence HNO₃ formation and deposition, a
33 variation by a factor of two may be expected.

1 The potential HONO emission fluxes from the photolysis of adsorbed HNO₃ were calculated
2 using three different approaches:

- 3 i) All measured nitrate represents adsorbed HNO₃ at the top surface of the needles, and
4 HONO formation from photolysis of adsorbed HNO₃ proceeds with an empirical
5 enhancement factor of 43 of $j(\text{HNO}_3)$ (Zhou et al., 2011).
- 6 ii) Similar to i) but the nitrate loading is distributed over the whole geometric surface of
7 the needles (Oren et al., 1986), thus, a factor of 2.65 less HNO₃ is exposed to
8 radiation.
- 9 iii) The photolysis frequency of adsorbed HNO₃ is calculated directly from the absorption
10 cross section of adsorbed HNO₃ on fused silica reported by Zhu et al. (2008) and the
11 corresponding irradiance calculated by the TUV model. This photolysis frequency
12 multiplied with the nitrate loading according to ii) yields the NO₂ formed at the
13 surface. Then, HONO formation is calculated as described in Sect. 3.4.2. To derive the
14 reactive uptake coefficient according to Eq. (2) (Stemmler et al., 2007) we used the
15 irradiance integrated over the 290-700 nm wavelength range and calculated the NO₂
16 concentration which is equivalent to the amount of NO₂ molecules formed at the
17 surface by HNO₃ photolysis.

18
19 A comparison of $j(\text{NO}_2)$ values from the TUV model with those calculated from global
20 radiation measurements by the approach of Trebs et al. (2009) showed a reasonable
21 agreement. The values agree within 8 % around noon.

22 Figure 5 summarizes the results of the different approaches. Based on empirical factors of
23 light enhancement and HONO formation (Zhou et al., 2011) approaches i) and ii) yielded a
24 light-dependent HONO source in the same order of magnitude as the estimated HONO fluxes
25 ($0.04 \pm 0.02 \text{ nmol m}^{-2} \text{ s}^{-1}$; see Sect. 3). The calculated potential HONO fluxes according to
26 approach i) are a factor of two higher (about $0.46 \text{ nmol m}^{-2} \text{ s}^{-1}$) than those of Zhou et al.
27 (2011) ($0.25 \text{ nmol m}^{-2} \text{ s}^{-1}$), which is consistent with the factor of two higher nitrate loading
28 measured at our site. However, we consider approach ii) to be more realistic. The diurnal
29 cycle of this source (Fig. 5) follows $j(\text{HNO}_3)$ as the mean nitrate loading is used for the
30 calculation. This seems to be valid as we found rather constant surface nitrate loadings during
31 different times of the day (see Fig. S4).

1 Approach iii), a combination of photolysis of adsorbed HNO₃ and light-induced conversion of
2 the photolysis product NO₂ (see also section 3.4.2) as proposed by Zhou et al. (2011), reveals
3 several interesting findings:

- 4 • The calculated photolysis frequency of adsorbed HNO₃ is higher than in the gas phase
5 by a factor of 2000.
- 6 • The lifetime of adsorbed HNO₃ with respect to photolysis is only about 15 min at
7 noon.
- 8 • NO₂ formed at the surface by HNO₃ photolysis corresponds to a mixing ratio of NO₂
9 in the gas phase of only a few ppt.

10 If the strongly enhanced photolysis of adsorbed HNO₃ is valid for natural surfaces, this would
11 have important implications for HNO₃ deposition. HNO₃ would most likely be an
12 intermediate with a lifetime comparable to that of HONO (about 15 min at noon) than a final
13 sink for NO_x. However, even if photolysis of adsorbed HNO₃ is strongly enhanced, formation
14 of HONO would be rather slow if the subsequent reaction of NO₂* (Abida et al., 2012) occurs
15 via the light-induced NO₂ conversion (Stemmler et al., 2006) as proposed by Zhou et al.
16 (2011). As shown in sect. 3.4.2 the light induced conversion is light saturated during most of
17 the day especially for low NO₂ mixing ratios. If we compare the number NO₂ molecules
18 formed at the surface through HNO₃ photolysis to the number of NO₂ molecules hitting the
19 surface through gas kinetic collisions this would correspond to a mixing ratio of a few ppt
20 only. Thus, this pathway would not compete with ambient NO₂ for the conditions in our
21 study. Hence, a different NO₂* reaction mechanism to explain the proposed HONO formation
22 from HNO₃ must exist. A potential pathway for NO₂* to form HONO would be the reaction
23 with water (e.g., Crowley and Carl 1997; Amedro et al., 2011). Sörgel et al. (2011a)
24 speculated that the reaction of NO₂* with water at the surface might be faster than the
25 respective gas phase reaction, which is not of atmospheric importance (e.g., Crowley and Carl
26 1997; Sörgel et al., 2011a; Amedro et al., 2011). The formation of NO₂* (either from HNO₃
27 photolysis or directly in the gas phase) is not the limiting step, as in the gas phase *j* values for
28 excitation (NO₂ => NO₂*) are about a factor of five higher under typical tropospheric
29 conditions (Crowley and Carl, 1997) than for photo dissociation of NO₂. The limiting step is
30 the small portion of reactive quenching of NO₂* by water vapour as the majority of excited
31 NO₂ molecules gets deactivated by collision with N₂, O₂ and water vapour. According to
32 Abida et al. (2012), deactivation of NO₂* is much faster at the surface than in the gas phase,
33 thus reducing the probability for reactive quenching with water and formation of HONO. For

1 a quantitative evaluation of this reaction pathway, knowledge of the ratio of deactivation to
2 reactive quenching of surface adsorbed NO_2^* and H_2O is crucial. Another pathway might be
3 the photolysis of nitrate in aqueous solution that has been reported to yield HONO and NO_2
4 (Scharko et al. 2014), whereby HONO formation was attributed to efficient hydrolysis of NO_2
5 that is formed in solution.

7 ***3.5 Comparison of calculated fluxes and source estimates***

8
9 Transferring the HONO formation mechanisms proposed from laboratory measurements to
10 field conditions involves uncertainties as discussed in detail in the previous sections.
11 However, except for HNO_3 photolysis (Zhou et al., 2011) these source mechanisms have not
12 been quantified in field studies up to now. Furthermore, to our knowledge the various
13 reactions have not been studied under natural conditions, except for a proof of principle with
14 irradiated bare soil as a natural humic acid environment (Stemmler et al., 2006), and the
15 empirically derived HNO_3 conversion factors (Zhou et al., 2003). In Figure 6 all source
16 estimates and the observed flux estimates from the field are summarized. The main findings
17 are a) that all sources are within the same order of magnitude, and b) due to the large
18 systematic uncertainties of the source estimates and the potentially large errors of the flux
19 estimates, none of the sources can be favoured or excluded.

20 The soil flux was the only source to be measured directly, and these measurements were
21 performed in the laboratory. The soil HONO flux would likely be lower in the field as the soil
22 at the site was covered by vegetation which can take up HONO (Schimang et al., 2006) and
23 because ambient HONO mixing ratios were above zero. NO_2 mixing ratios dropped below
24 500 ppt in the afternoon, leading to very low HONO fluxes from light-induced NO_2
25 conversion. Surprisingly, this photochemical source did not show a diurnal cycle but became
26 light-saturated early in the morning and, thus, was solely dependent on NO_2 mixing ratios. It
27 remains an open question whether light saturation occurs also on natural surfaces. The
28 photolysis of adsorbed HNO_3 produced considerable HONO fluxes ((even for case ii), Sect.
29 3.4.3) when using an empirically derived HONO conversion factor (Zhou et al., 2003; Zhou et
30 al., 2011). In contrast, the proposed mechanism based on reaction kinetics ((case iii), Sect.
31 3.4.3) failed to produce considerable amounts of HONO. Although some of the sources were
32 unexpectedly small, the combination of all three sources yields much higher fluxes than
33 measured in the field. This may be attributed to enhanced deposition of HONO during the day

1 due to stomata opening and take-up by plants (Schimang et al., 2006), which would reduce
2 measured net emission fluxes. However, the contribution of daytime deposition has not been
3 measured up to now.

4 **4 Conclusions**

5 Our results reveal that the forest floor was predominantly a net sink for HONO, and the
6 clearing constitutes a net sink for HONO during nighttime and a net source during daytime.
7 Hence, net sources and net sinks coexist in heterogeneous landscapes.

8 HONO emissions calculated for three proposed mechanisms agreed with the measured fluxes
9 within one order of magnitude. On the one hand, this shows that the postulated sources are of
10 the right order of magnitude, but on the other hand, even the presented comprehensive data
11 set including vertical profiles is not sufficient to exclude or confirm one individual source.
12 The detailed investigation of three potential HONO sources, i.e., soil emissions, NO₂
13 conversion with humic acids and photolysis of adsorbed HNO₃, revealed important findings:

14

- 15 • Soil emissions were found to be several orders of magnitude lower than expected from
16 the model of Su et al. (2011), and calculated fluxes are very sensitive to the
17 parameterization of mass transfer from the soil to the atmosphere. Furthermore, acidic
18 soils do not necessarily favour HONO emissions. Emissions are a factor of 700 higher
19 for agricultural soils (Oswald et al., 2013), thus emissions might be highly influenced
20 by microbial activities.
- 21 • NO₂ conversion on humic acid surfaces was found to be light-saturated from the early
22 morning throughout most of the daytime under ambient conditions and, thus, only
23 dependent on NO₂. This saturation effect has not been observed in field measurements
24 up to now. Consequently, we could not identify the expected correlation of HONO
25 formation with $j(\text{NO}_2)$ for this reaction. Furthermore, at low NO₂ levels this source is
26 very small at our site.
- 27 • Photolysis of adsorbed HNO₃ was found to explain the estimated HONO fluxes when
28 using an empirical parameterization for HONO formation, but it failed to produce
29 noticeable amounts of HONO when the formation was calculated according to the
30 proposed mechanism and literature values for adsorption cross sections and reaction
31 kinetics.

1 Since HNO₃ photolysis is not correlated to $j(\text{NO}_2)$ either, the correlation of the unknown
2 HONO source to $j(\text{NO}_2)$ as observed for example by Su et al. (2008) and Sörgel et al. (2011a)
3 might originate from the unbalanced photolytic loss term of HONO ($j(\text{HONO})_x[\text{HONO}]$).
4 This loss term is highly correlated to $j(\text{NO}_2)$ in the budget calculations (Oswald et al., 2014),
5 and is generally interpreted as the unknown source. Recently, an internal source of HONO in
6 the boundary layer from the interconversion between NO_x and HO_x has been postulated with a
7 contribution of about 75 % (Li et al., 2014). Such a source would explain the observed
8 correlation to $j(\text{NO}_2)$ or $j(\text{HONO})$. In our study, the surface emission flux of HONO is only in
9 the order of a few per cent of the calculated photolytic loss within the boundary layer, which
10 is even less than estimated from boundary layer profile measurements (~20 % ground
11 contribution; Zhang et al., 2009; Li et al., 2014).

12 However, a daytime ground source of HONO exists that can produce additional OH, thus
13 enhancing the oxidation capacity of the lower troposphere. The relative contributions of
14 ground sources and volume sources and, hence, the contribution of HONO to primary OH
15 formation remains to be quantified by combining field measurements with the application of
16 chemistry and transport models.

17

18 **Acknowledgements:**

19 The authors gratefully acknowledge financial support by the German Science Foundation
20 (DFG project HE 5214/4-1) and by the Max Planck Society. We would like to acknowledge
21 the Department for Micrometeorology of the University of Bayreuth for the eddy flux
22 measurements during IOP-3 and the meteorological data from the “Pflanzgarten”-site.
23 Groundcover types and plant area data are courtesy of Eva Falge and Linda Voss. We are
24 grateful to Robert Oswald for checking and assisting with the calculations regarding the soil
25 emissions. Erica Duran helped with the nitrate loading sampling and calculated the needle
26 areas. We thank Tracey Andreae for proofreading the manuscript.

27

28 **References:**

29

- 30 Abida, O., Du, J., and Zhu, L.: Investigation of the photolysis of the surface-adsorbed HNO₃
31 by combining laser photolysis with Brewster angle cavity ring-down spectroscopy,
32 Chem. Phys. Lett., 534, 77–82, 2012.
33 Alicke, B., Geyer, A., Hofzumahaus, A., Holland, F., Konrad, S., Pätz, H. W., Schäfer, J.,
34 Stutz, J., Volz-Thomas, A., and Platt, U.: OH formation by HONO photolysis during

1 the BERLIOZ experiment, *J. Geophys. Res.*, 108, 8247, doi:10.1029/2001JD000579,
2 2003.

3 Allison F.: Losses of gaseous nitrogen from soils by chemical mechanisms involving nitrous
4 acid and nitrites. *Soil Sci.*, 96, 404–409, 1963.

5 Amedro, D., Parker, A. E., Schoemaeker, C., and Fittschen, C.: Direct observation of OH
6 radicals after 565 nm multi-photon excitation of NO₂ in the presence of H₂O, *Chem.*
7 *Phys. Lett.*, 513, 12–16, 2011.

8 Arens, F., Gutzwiller, L., Baltensperger, U. r., Gäggler, H. W., and Ammann, M.:
9 Heterogeneous reaction of NO₂ on diesel soot particles, *Environ. Sci. Technol.*, 35,
10 2191-2199, 2001.

11 Aubin, D. G., and Abbatt, J. P. D.: Interaction of NO₂ with hydrocarbon soot: focus on
12 HONO yield, surface modification, and mechanism, *J. Phys. Chem. A*, 111, 6263-
13 6273, 2007.

14 Bargsten, A., Falge, E., Pritsch, K., Huwe, B., and Meixner, F. X.: Laboratory measurements
15 of nitric oxide release from forest soil with a thick organic layer under different
16 understory types, *Biogeosciences*, 7, 1425–1441, doi:10.5194/bg-7-1425-2010, 2010.

17 Bartels-Rausch, T., Brigante, M., Elshorbany, Y. F., Ammann, M., D'Anna, B., George, C.,
18 Stemmler, K., Ndour, M. and Kleffmann, J.: Humic acid in ice: Photo-enhanced
19 conversion of nitrogen dioxide into nitrous acid, *Atmos. Environ.*, 44, 5443-5450,
20 2010.

21 Bejan, I., Aal, Y. A. E., Barnes, I., Benter, T., Bohn, B., Wiesen, P., and Kleffmann, J.: The
22 photolysis of ortho-nitrophenols: a new gas phase source of HONO, *Phys. Chem.*
23 *Chem. Phys.*, 8, 2028–2035, DOI: 10.1039/b516590c, 2006.

24 Clark, F.E.: Losses of nitrogen accompanying nitrification. *Transactions of the International*
25 *Society of Soil Science, Communications IV and V*, pp. 173-176, 1962.

26 Colussi, A. J., Enami, S., Yabushita, A., Hoffmann, M. R., Liu, W.-G., Mishraaf, H., and
27 Goddard, W. A.: Tropospheric aerosol as a reactive intermediate, *Faraday Discuss.*,
28 165, 407–420, 2013.

29 Cox, R. A.: The photolysis of nitrous acid in the presence of carbon monoxide and sulphur
30 dioxide, *J. Photochem.*, 3, 291 - 304, 1974.

31 Crowley, J., N., and Carl, S., A.: OH formation in the photoexcitation of NO₂ beyond the
32 dissociation threshold in the presence of water vapor, *J. Phys. Chem. A*, 101, 4178-
33 4184, 1997.

34 De Boer, W. and Kowalchuk, G.A.: Nitrification in acid soils: micro-organisms and
35 mechanisms, *Soil Biol. Biochem.*, 33, 853-866, 2001.

36 De Jesus Medeiros, D., and Pimentel, A. S.: New insights in the atmospheric HONO
37 formation: New pathways for N₂O₄ isomerization and NO₂ dimerization in the
38 presence of water, *Journal of Physical Chemistry A*, 115, 6357-6365, 2011.

39 Donaldson, M. A., Berke, A. E., and Raff, J. D.: Uptake of Gas Phase Nitrous Acid onto
40 Boundary Layer Soil Surfaces, *Environ. Sci. Technol.*, 48, 375–383, DOI:
41 10.1021/es404156a, 2014a.

42 Donaldson, M. A., Bish, D. L., and Raff, J. D.: Soil surface acidity plays a determining role in
43 the atmospheric-terrestrial exchange of nitrous acid, *P Natl Acad Sci USA*, 111,
44 18472–18477, doi: 10.1073/pnas.1418545112, 2014b.

45 Febo, A., Perrino, C., and Allegrini, I.: Measurement of nitrous acid in Milan, Italy, by DOAS
46 and diffusion denuders, *Atmos. Environ.*, 30 3599-3609, 1996.

47 Finlayson-Pitts, B. J., Wingen, L. M., Sumner, A. L., Syomin, D., and Ramazan, K. A.: The
48 heterogeneous hydrolysis of NO₂ in laboratory systems and in outdoor and indoor
49 atmospheres: An integrated mechanism, *Phys. Chem. Chem. Phys.*, 5, 2003.

- 1 Finlayson-Pitts, B. J.: Reactions at surfaces in the atmosphere: integration of experiments and
2 theory as necessary (but not necessarily sufficient) for predicting the physical
3 chemistry of aerosols, *Phys. Chem. Chem. Phys.*, 11, 7760–7779, 2009.
- 4 Foken, T.: Lufthygienisch-bioklimatische Kennzeichnung des oberen Egertales
5 (Fichtelgebirge bis Karlovy Vary). *Bayreuther Forum Ökologie*, 100, Bayreuth, 70
6 pp., 2003.
- 7 Foken, T.: *Micrometeorology*, Springer, Heidelberg, 308 pp., 2008.
- 8 Foken, T., Meixner, F. X., Falge, E., Zetzsch, C., Serafimovich, A., Bargsten, A., Behrendt,
9 T., Biermann, T., Breuninger, C., Dix, S., Gerken, T., Hunner, M., Lehmann-Pape, L.,
10 Hens, K., Jocher, G., Kesselmeier, J., Lüers, J., Mayer, J.-C., Moravek, A., Plake, D.,
11 Riederer, M., Rütz, F., Scheibe, M., Siebicke, L., Sörgel, M., Staudt, K., Trebs, I.,
12 Tsokankunku, A., Welling, M., Wolff, V., and Zhu, Z.: Coupling processes and
13 exchange of energy and reactive and non-reactive trace gases at a forest site – results
14 of the EGER experiment, *Atmos. Chem. Phys.*, 12, 1923–1950, doi:10.5194/acp-12-
15 1923-2012, 2012.
- 16 George, C., Streckowski, R. S., Kleffmann, J., Stemmler, K., and Ammann, M.:
17 Photoenhanced uptake of gaseous NO₂ on solid organic compounds: a photochemical
18 source of HONO?, *Faraday Discuss.*, 130, 195–210, 2005.
- 19 Gustafsson, R. J., Kyriakou, G., and Lambert, R. M.: The molecular mechanism of
20 tropospheric nitrous acid production on mineral dust surfaces, *ChemPhysChem*, 9,
21 1390–1393, 2008.
- 22 Gutzwiller, L., George, C., Rössler, E., and Ammann, M.: Reaction kinetics of NO₂ with
23 resorcinol and 2,7-naphthalenediol in the aqueous phase at different pH, *J. Phys.*
24 *Chem. A*, 106, 12045–12050, 2002. Harrison, R. M., and Kitto, A.-M. N.: Evidence for
25 a surface source of atmospheric nitrous acid, *Atmos. Environ.*, 28, 1089–1094, 1994.
- 26 Harrison, R. M., Peak, J. D., and Collin, G. M.: Tropospheric cycle of nitrous acid, *J.*
27 *Geophys. Res.*, 101, 14429–14439, 1996.
- 28 Heland, J., Kleffmann, J., Kurtenbach, R., and Wiesen, P.: A new instrument to measure
29 gaseous nitrous acid (HONO) in the atmosphere, *Environ. Sci. Technol.*, 35, 3207–
30 3212, 2001.
- 31 Kamboures, M. A., Raff, J. D., Miller, Y., Phillips, L. F., Finlayson-Pitts, B. J., and Gerber,
32 R. B.: Complexes of HNO₃ and NO₃ with NO₂ and N₂O₄, and their potential role in
33 atmospheric HONO formation, *Phys. Chem. Chem. Phys.*, 10, 6019–6032, 2008.
- 34 Kleffmann, J., Becker, K. H., Lackhoff, M., and Wiesen, P.: Heterogeneous conversion of
35 NO₂ on carbonaceous surfaces, *Phys. Chem. Chem. Phys.*, 1, 5443–5450, 1999.
- 36 Kleffmann, J., Heland, J., Kurtenbach, R., Lörzer, J., and Wiesen, P.: A new instrument
37 (LOPAP) for the detection of nitrous acid (HONO), *Environ. Sci. Pollut. R.*, 4, 48–54,
38 2002.
- 39 Kleffmann, J., Gavriloaiei, T., Hofzumahaus, A., Holland, F., Koppmann, R., Rupp, L.,
40 Schlosser, E., Siese, M., and Wahner, A.: Daytime formation of nitrous acid: A major
41 source of OH radicals in a forest, *Geophys. Res. Lett.*, 32, 2005.
- 42 Kleffmann, J.: Daytime sources of nitrous acid (HONO) in the atmospheric boundary layer,
43 *ChemPhysChem*, 8, 1137 – 1144, 2007.
- 44 Kubota, M. and Asami, T.: Source of nitrous acid volatilized from upland soils, *Soil Sci. Plant*
45 *Nutr.*, 31, 35–42, 1985.
- 46 Lee, B.H, Wood, E. C., Herndon, S. C., Lefer, B. L., Luke, W. T., Brune, W. H., Nelson, D.
47 D., Zahniser, M. S. and Munger, J. W.: Urban measurements of atmospheric nitrous
48 acid: A caveat on the interpretation of the HONO photostationary state, *J. Geophys.*
49 *Res.*, 118, 1–8, doi:10.1002/2013JD020341, 2013.

- 1 Li, X., Rohrer, F., Hofzumahaus, H., Brauers, T., Häseler, R., Bohn, B., Broch, S., Fuchs, H.,
2 Gomm, S., Holland, F., Jäger, J., Kaiser, J., Keutsch, F. N., Lohse, I., Lu, K.,
3 Tillmann, R., Wegener, R., Wolfe, G. M., F. Mentel, T. F., Kiendler-Scharr, A. and
4 Wahner, A.: Missing gas-phase source of HONO inferred from zeppelin
5 measurements in the troposphere, *Science*, 344, 292, 2014.
- 6 Ludwig, J., Meixner, F. X., Vogel, B. and Förstner J.: Soil-air exchange of nitric oxide: An
7 overview of processes, environmental factors, and modeling studies, *Biogeochemistry*,
8 52, 225–257, 2001.
- 9 Madronich, S. and Flocke, S., The role of solar radiation in atmospheric chemistry, in *The*
10 *Handbook of Environmental Chemistry / Reactions and Processes / Environmental*
11 *Photochemistry Part I: BD 2 / Part L*, Boule, P. (ed.), Springer-Verlag, Heidelberg,
12 373 (pp. 1-26), 1998.
- 13 Maljanen, M., Yli-Pirilä, P., Hytönen, J., Joutsensaari, J., and Martikainen, P. J.: Acidic
14 northern soils as sources of atmospheric nitrous acid (HONO), *Soil Biol. Biochem.*,
15 67, 94–97, DOI: 10.1016/j.soilbio.2013.08.013, 2013.
- 16 Matthies, C., Erhard, H.-P., Drake, H.L.: Effects of pH on the comparative culturability of
17 fungi and bacteria from acidic and less acidic forest soils, *J. Basic. Microb.*, 37, 335-
18 343, 1997.
- 19 Mauder, M. and Foken, T.: Documentation and instruction manual of the eddy-covariance
20 software package TK3, Universität Bayreuth, Abteilung Mikrometeorologie, 46, 60
21 pp., ISSN1614-8924, 2011.
- 22 Miller, Y., Finlayson-Pitts, B. J., and Gerber, R. B.: Ionization of N₂O₄ in contact with water:
23 mechanism, time scales and atmospheric implications, *J. Am. Chem. Soc.*, 131,
24 12180–12185, DOI: 10.1021/ja900350g, 2009.
- 25 Moldrup, P., Olesen, T., Gamst, J., Schjonning, P., Yamaguchi, T., and Rolston, D. E.:
26 Predicting the gas diffusion coefficient in repacked soil: Water-induced linear
27 reduction model, *Soil Science Society of America Journal*, 64, 1588-1594, 2000.
- 28 Oswald, R., Behrendt, T., Ermel, M., Wu, D., Su, H., Cheng, Y., Breuninger, C., Moravek,
29 A., Mougou, Delon, C., Loubet, B., Pommerening-Röser, A., Sörgel, M., Pöschl, U.,
30 Hoffmann, T., Andreae, M.O., Meixner, F.X. and Trebs, I.: HONO emissions from
31 soil bacteria as a major source of atmospheric reactive Nitrogen, *Science*, 341, 1233-
32 1235, DOI: 10.1126/science.1242266, 2013.
- 33 Oswald, R., Ermel, M., Hens, K., Novelli, A., Ouwersloot, H. G., Paasonen, P., Petäjä, T.,
34 Sipilä, M., Keronen, P., Bäck, J., Königstedt, R., Hosaynali Beygi, Z., Fischer, H.,
35 Bohn, B., Kubistin, D., Harder, H., Martinez, M., Williams, J., Hoffmann, T., Trebs,
36 I., and Sörgel, M.: Comparison of HONO budgets for two measurement heights at a
37 field station within the boreal forest (SMEAR II – HUMPPA-COPEC 2010), *Atmos.*
38 *Chem. Phys. Discuss.*, 14, 7823-7857, doi:10.5194/acpd-14-7823-2014, 2014.
- 39 Oren, R., Schulze, E.-D., Matyssek, R., and Zimmermann, R.: Estimating photosynthetic rate
40 and annual carbon gain in conifers from specific leaf weight and leaf biomass,
41 *Oecologia*, 70, 187– 193, 1986.
- 42 Pape, L., Ammann, C., Nyfeler-Brunner, A., Spirig, C., Hens, K., and Meixner, F. X.: An
43 automated dynamic chamber system for surface exchange measurement of non-
44 reactive and reactive trace gases of grassland ecosystems, *Biogeosciences*, 6, 405-429,
45 doi:10.5194/bg-6-405-2009, 2009.
- 46 Ramazan, K. A., Syomin, D., Finlayson-Pitts, B. J.: The photochemical production of HONO
47 during the heterogeneous hydrolysis of NO₂. *Phys. Chem. Chem. Phys.*, 6, 3836-3843,
48 2004.
- 49 Ren, X., Sanders, J. E., Rajendran, A., Weber, R. J., Goldstein, A. H., Pusede, S. E., Browne,
50 E. C., Min, K.-E., and Cohen, R. C.: A relaxed eddy accumulation system for

1 measuring vertical fluxes of nitrous acid, *Atmos. Meas. Tech.*, 4, 2093-2103,
2 doi:10.5194/amt-4-2093-2011, 2011.

3 Rousk, J., Bååth, E., Brookes, P.C., Lauber, C.L., Lozupone, C., Caporaso, J.G., Knight, R.,
4 and Fierer, N.: Soil bacterial and fungal communities across a pH gradient in an arable
5 soil, *ISME J.*, 4, 1340–1351, 2010.

6 Rubasinghege, G., and Grassian V. H.: Photochemistry of adsorbed nitrate on aluminum
7 oxide particle surfaces, *J. Phys. Chem. A*, 113, 7818–7825, 2009.

8 Scharko, N. K., Berke, A. E., and Raff, J. D.: Release of nitrous acid and nitrogen dioxide
9 from nitrate photolysis in acidic aqueous solutions, *Environ. Sci. Technol.*, 48, 11991–
10 12001, doi: 10.1021/es503088x, 2014.

11 Schimang R., Folkers A., Kleffmann J., Kleist E., Miebach M., Wildt J.: Uptake of Gaseous
12 Nitrous Acid (HONO) by Several Plant Species, *Atmos. Environ.*, 40, 1324-1335,
13 2006.

14 Schuttlefield, J., Rubasinghege, G., El-Maazawi, M., Bone, J., and Grassian V. H.:
15 Photochemistry of adsorbed nitrate, *J. Am. Chem. Soc.*, 130, 12210–12211, 2008.

16 Sörgel, M., Regelin, E., Bozem, H., Diesch, J.-M., Drewnick, F., Fischer, H., Harder, H.,
17 Held, A., Hosaynali-Beygi, Z., Martinez, M., and Zetzsch, C.: Quantification of the
18 unknown HONO daytime source and its relation to NO₂, *Atmos. Chem. Phys.*, 11,
19 10433-10447, doi:10.5194/acp-11-10433-2011, 2011a.

20 Sörgel, M., Trebs, I., Serafimovich, A., Moravek, A., Held, A., and Zetzsch, C.: Simultaneous
21 HONO measurements in and above a forest canopy: influence of turbulent exchange
22 on mixing ratio differences, *Atmos. Chem. Phys.*, 11, 841-855, doi:10.5194/acp-11-
23 841-2011, 2011b.

24 Stemmler, K., Ammann, M., Donders, C., Kleffmann, J., and George, C.: Photosensitized
25 reduction of nitrogen dioxide on humic acid as a source of nitrous acid, *Nature*, 440,
26 195-198, 2006.

27 Stemmler, K., Ammann, M., Elshorbany, Y., Kleffmann, J., Ndour, M., D’Anna, B., George,
28 C., and Bohn, B.: Light induced conversion of nitrogen dioxide into nitrous acid on
29 submicron humic acid aerosol, *Atmos. Chem. Phys.*, 7, 4237–4248, 2007.

30 Stutz, J., Alicke, B., and Neftel, A.: Nitrous acid formation in the urban atmosphere: Gradient
31 measurements of NO₂ and HONO over grass in Milan, Italy, *J. Geophys. Res.*, 107
32 doi:10.1029/2001JD000390, 2002.

33 Su, H., Cheng, Y. F., Shao, M., Gao, D. F., Yu, Z. Y., Zeng, L. M., Slanina, J., Zhang, Y. H.,
34 and Wiedensohler, A.: Nitrous acid (HONO) and its daytime sources at a rural site
35 during the 2004 PRIDE-PRD experiment in China, *J. Geophys. Res.*, 113,
36 doi:10.1029/2007JD009060, 2008.

37 Su, H., Cheng, Y., Oswald, R., Behrendt, T., Trebs, I., Meixner, F.-X., Andreae, M. O.,
38 Cheng, P., Zhang, Y., and Pöschl, U.: Soil nitrite as a source of atmospheric HONO
39 and OH radicals, *Science*, 333, 1616–1618, doi:10.1126/science.1207687, 2011.

40 Trebs, I., Bohn, B., Ammann, C., Rummel, U., Blumthaler, M., Königstedt, R., Meixner, F.
41 X., Fan, S., and Andreae, M. O.: Relationship between the NO₂ photolysis frequency
42 and the solar global irradiance, *Atmos. Meas. Tech.*, 2, 725–739, 2009.

43 Van Cleemput, O. and Baert, L.: Nitrite: a key compound in N loss processes under acid
44 conditions?, *Plant Soil*, 76, 233-241, 1984.

45 VandenBoer, T. C., Brown, S. S., Murphy, J. G., Keene, W. C., Young, C. J., Pszenny, A. A.
46 P., Kim, S., Warneke, C., de Gouw, J. A., Maben, J. R., Wagner, N. L., Riedel, T. P.,
47 Thornton, J. A., Wolfe, D. E., Dubé, W. P., Öztürk, F., Brock, C. A., Grossberg, N.,
48 Lefter, B., Lerner, B., Middlebrook, A. M., and Roberts, J. M.: Understanding the role
49 of the ground surface in HONO vertical structure: High resolution vertical profiles

1 during NACHTT-11, *Journal of Geophysical Research: Atmospheres*, 118, 10,155-
2 110,171, 10.1002/jgrd.50721, 2013.

3 VandenBoer, T. C., Young, C. J., Talukdar, R. K., Markovic, M. Z., Brown, S. S., Roberts, J.
4 M., and Murphy, J. G.: Nocturnal loss and daytime source of nitrous acid through
5 reactive uptake and displacement, *Nat. Geosci.*, 8, 5-7, doi:10.1038/ngeo2315, 2015.

6 Venterea, R.T., Rolston, D.E., and Cardon, Z.G.: Effects of soil moisture, physical, and
7 chemical characteristics on abiotic nitric oxide production, *Nutr. Cycl. Agroecosys.*,
8 72, 27–40, 2005.

9 Volkamer, R., Sheehy, P., Molina, L. T., and Molina, M. J.: Oxidative capacity of the Mexico
10 City atmosphere – Part 1: A radical source perspective, *Atmos. Chem. Phys.*, 10,
11 6969–6991, doi:10.5194/acp-10-6969-2010, 2010.

12 Wolff, V., Trebs, I., Ammann, C., and Meixner, F. X.: Aerodynamic gradient measurements
13 of the NH₃-HNO₃-NH₄NO₃ triad using a wet chemical instrument: an analysis of
14 precision requirements and flux errors, *Atmos. Meas. Tech.*, 3, 187-208,
15 doi:10.5194/amt-3-187-2010, 2010.

16 Wong, K. W., Oh, H.-J., Lefer, B. L., Rappenglück, B., and Stutz, J.: Vertical profiles of
17 nitrous acid in the nocturnal urban atmosphere of Houston, TX, *Atmos. Chem. Phys.*,
18 11, 3595-3609, doi:10.5194/acp-11-3595-2011, 2011.

19 Wong, K. W., Tsai, C., Lefer, B., Haman, C., Grossberg, N., Brune, W. H., Ren, X., Luke,
20 W., and Stutz, J.: Daytime HONO vertical gradients during SHARP 2009 in Houston,
21 TX, *Atmos. Chem. Phys.*, 12, 635-652, doi:10.5194/acp-12-635-2012, 2012.

22 Wong, K. W., Tsai, C., Lefer, B., Grossberg, N., and Stutz, J.: Modeling of daytime HONO
23 vertical gradients during SHARP 2009, *Atmos. Chem. Phys.*, 13, 3587-3601,
24 10.5194/acp-13-3587-2013, 2013.

25 Yabushita, A., Enami, S., Sakamoto, Y., Kawasaki, M., Hoffmann, M. R., and Colussi, A. J.:
26 Anion-catalyzed dissolution of NO₂ on aqueous microdroplets, *J. Phys. Chem. A*, 113,
27 4844–4848, 2009.

28 Zhang, N., Zhou, X., Shepson, P. B., Gao, H., Alaghmand, M., and Stirm, B.: Aircraft
29 measurement of HONO vertical profiles over a forested region, *Geophys. Res. Lett.*,
30 36, L15820, doi:10.1029/2009GL038999, 2009.

31 Zhang, N., Zhou, X., Bertman, S., Tang, D., Alaghmand, M., Shepson, P. B., and Carroll, M.
32 A.: Measurements of ambient HONO concentrations and vertical HONO flux above a
33 northern Michigan forest canopy, *Atmos. Chem. Phys.*, 12, 8285-8296,
34 doi:10.5194/acp-12-8285-2012, 2012.

35 Zhou, X., He, Y., Huang, G., Thornberry, T. D., Carroll, M. A., and Bertman, S. B.:
36 Photochemical production of nitrous acid on glass sample manifold surface, *Geophys.*
37 *Res. Lett.*, 29, 1681, 10.1029/2002GL015080, 2002.

38 Zhou, X., Gao, H., He, Y., Huang, G., Bertman, S. B., Civerolo, K., and Schwab, J.: Nitric
39 acid photolysis on surfaces in low-NO_x environments: Significant atmospheric
40 implications, *Geophys. Res. Lett.*, 30, 1-4, 2003.

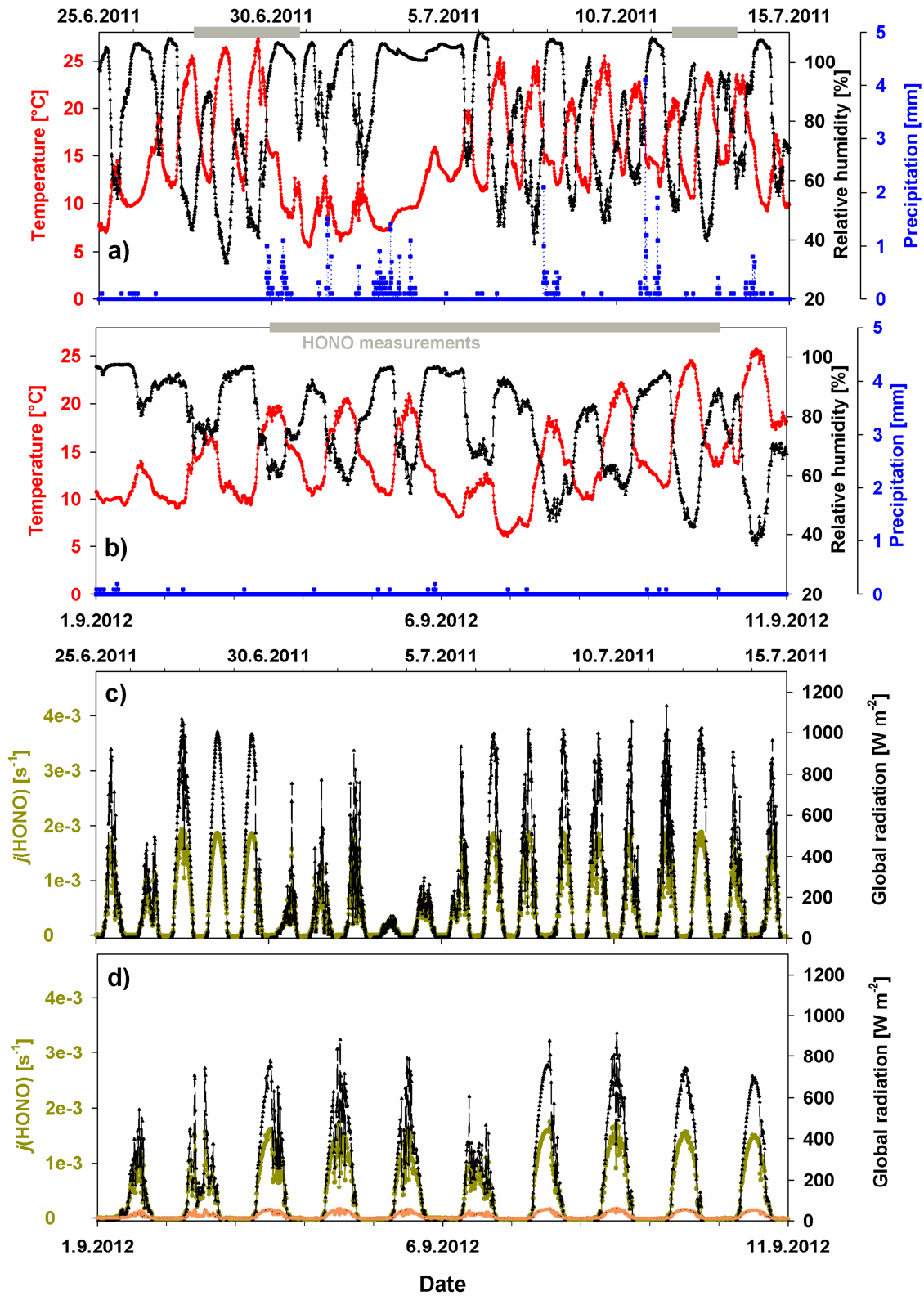
41 Zhou, X. L., Zhang, N., TerAvest, M., Tang, D., Hou, J., Bertman, S., Alaghmand, M.,
42 Shepson, P. B., Carroll, M. A., Griffith, S., Dusanter, S., and Stevens, P. S.: Nitric acid
43 photolysis on forest canopy surface as a source for tropospheric nitrous acid, *Nat.*
44 *Geosci.*, 4, 440-443, 10.1038/ngeo1164, 2011.

45 Zhu, C., Xiang, B., Zhu, L., Cole, R.: Determination of absorption cross sections of surface-
46 adsorbed HNO₃ in the 290–330 nm region by Brewster angle cavity ring-down
47 spectroscopy, *Chem. Phys. Lett.*, 458, 73–377, 2008.

48 Zhu, C., Xiang, B., Chu, L. T. and Zhu, L.: Photolysis of Nitric Acid in the Gas Phase, on
49 Aluminum Surfaces, and on Ice Films, *J. Phys. Chem. A*, 114, 2561–2568, 2010.

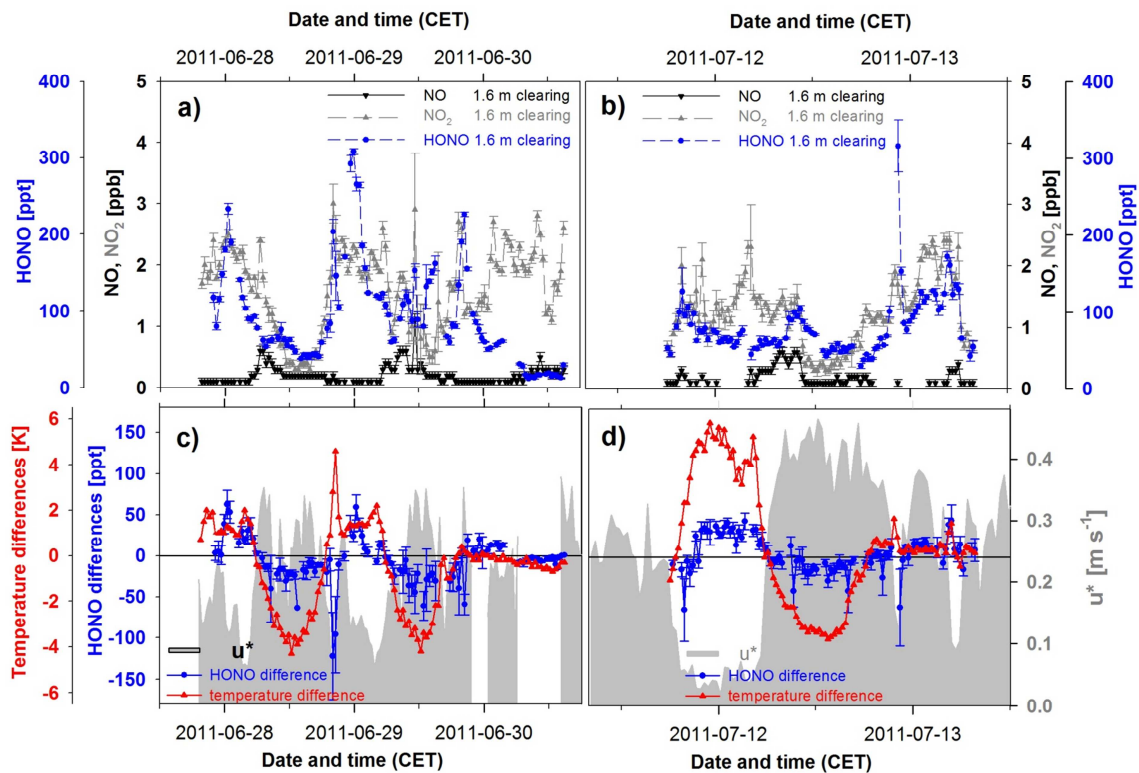
50

1
2

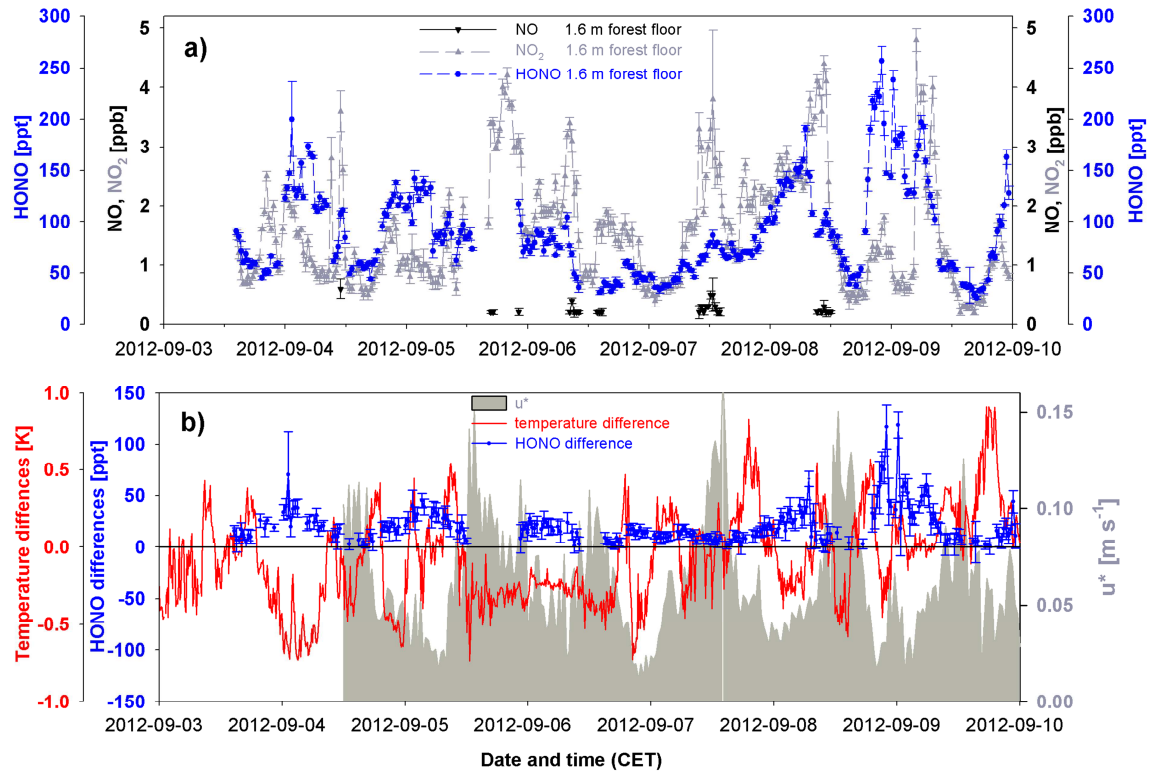


3

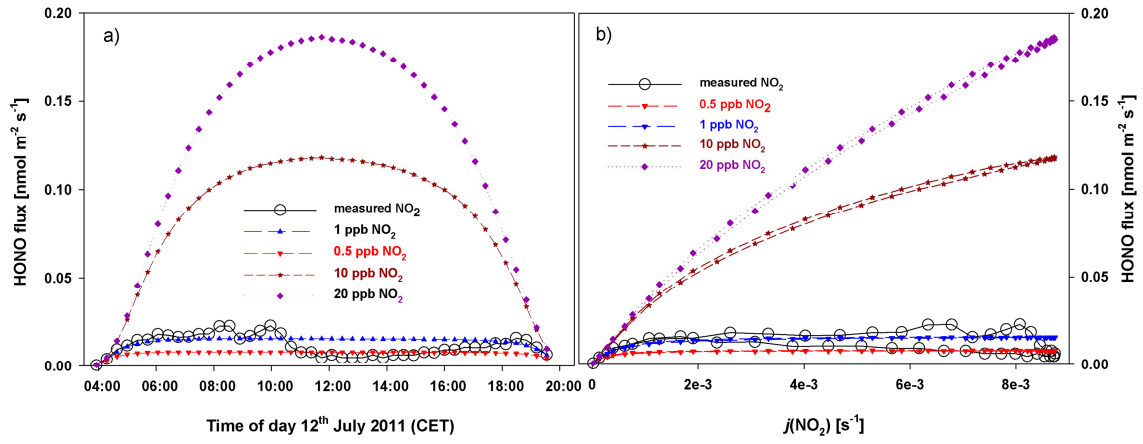
1 Figure 1: Temperature (red), relative humidity (RH, black) and precipitation (blue) averaged for a 10 min
 2 interval are shown in panels a) for 25th June to 15th July 2011 (IOP-3), and b) for 1st September 2012 to 11th
 3 September 2012 (IOP-4). Periods when HONO vertical profiles were measured are indicated by grey bars at the
 4 top of the graphs. Panels c) and d) show solar global irradiance (black) and $j(\text{HONO})$ in dark yellow, calculated
 5 according to Trebs et al. (2009), for the respective campaigns. Additionally, $j(\text{HONO})$ at the forest floor (orange)
 6 was calculated by applying a factor of 10 taking into account attenuation by the canopy (cf. Sörgel et al., 2011b).
 7 All data were taken from the “Pflanzgarten” site.
 8
 9



10
 11 Figure 2: HONO (blue), NO (black) and NO₂ (grey) mixing ratios measured at the clearing at 1.6 m averaged for
 12 each height interval (i.e. omitting the first data points according to the time resolution of the instruments) from a)
 13 27 June to 30 June 2011 (NOx: 3.5 min mean; HONO: 3 min mean), and b) 11 July to 13 July 2011 (NOx: 4 min
 14 mean; HONO: 3 min mean). Missing NO values are below the detection limit ($\text{LOD}_{2\sigma} = 50$ ppt). Vertical
 15 temperature differences (red triangles and line) and HONO mixing ratio differences (blue dots and line) for each
 16 cycle (~ 30 min) are shown in c) and d) as well as the friction velocity (30 min mean) in grey shading.
 17 Differences of mean HONO values measured at 1.6 m and 0.1 m are presented and error bars denote combined
 18 standard deviations. For temperature, differences between 1.4 m and 0.1 m are shown.
 19

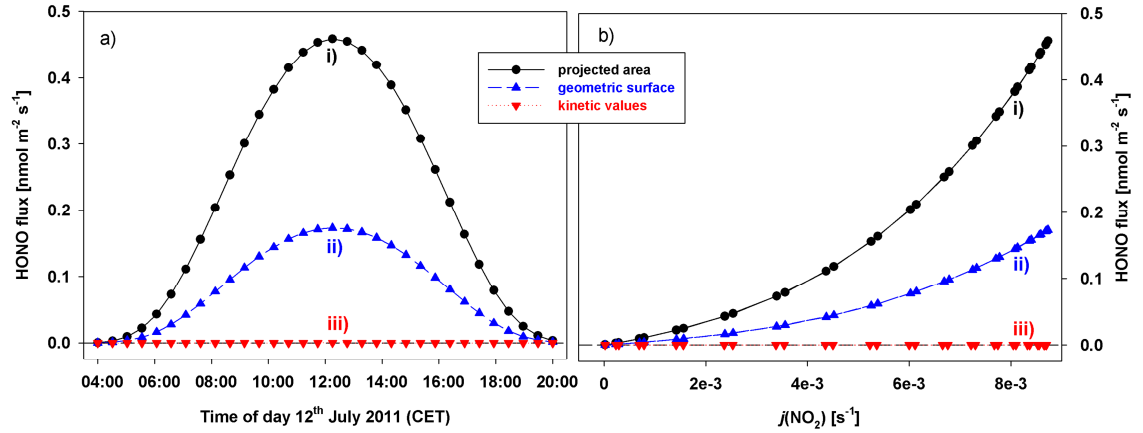


1
 2 Figure 3: HONO (blue), NO (black) and NO₂ (grey) mixing ratios measured at the forest floor at 1.6 m averaged
 3 for each height interval (i.e. omitting the first data points according to the time resolution of the instruments)
 4 from 3 September to 9 Sept 2012 (NOx: 7 min mean; HONO: 6 min mean) are shown in a). Missing NO values
 5 are below the detection limit ($LOD_{2\sigma} = 50$ ppt). Vertical temperature differences (red triangles and line) and
 6 HONO mixing ratio differences (blue dots and line) for each cycle (~ 30 min) are shown in b) as well as the
 7 friction velocity (30 min mean) in grey shading. Differences of mean HONO values measured at 1.6 m and 0.1
 8 m are presented and error bars denote combined standard deviations. For temperature, differences between 1.6 m
 9 and 0.1 m are shown.
 10



1
2
3
4
5
6

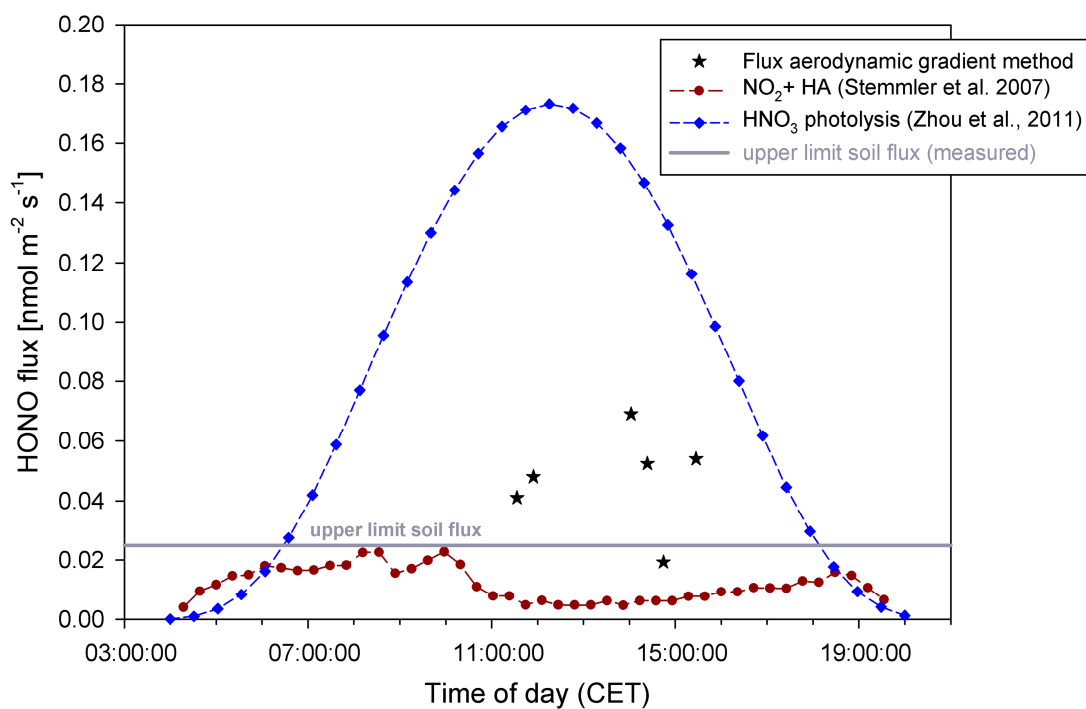
Figure 4: Diurnal cycles of HONO emission fluxes caused by light induced NO₂ conversion for different NO₂ mixing ratios are shown in a). The corresponding correlations of HONO formation with $j(\text{NO}_2)$ are presented in b).



7
8
9
10
11

Figure 5: HONO fluxes from photolysis of adsorbed HNO₃ calculated by three different approaches (for details see text). Diurnal cycles of the HONO fluxes are shown in a), whereas b) shows the relationship between HONO fluxes and $j(\text{NO}_2)$.

HONO fluxes at clearing (12th July 2011)



1

2 Figure 6: Comparison of measured HONO fluxes at the clearing on 12 July 2012 with estimates of potential
3 HONO sources. Black stars represent the fluxes derived from the aerodynamic gradient method. Blue diamonds
4 are HONO fluxes calculated from the measured nitrate loadings according to Zhou et al. (2011) but using the
5 geometric needle area (see Sect. 3.4.3, approach ii). Brown dots are calculated HONO fluxes according to
6 Stemmler et al. (2007) assuming a flat surface covered with humic acid. The grey horizontal line marks the
7 upper limit of soil HONO fluxes derived from laboratory dynamic chamber measurements.

8